JACS
JOURNAL OF THE AMERICAN CHEMICAL SOCIETY
Article
pubs.acs.org/JACS

Coinage Metals Binding as Main Group Elements: Structure and Bonding of the Carbene Complexes [TM(cAAC)$_2$] and [TM(cAAC)$_2$]$^+$ (TM = Cu, Ag, Au)

Paul Jerabek,[†] Herbert W. Roesky,*[,‡] Guy Bertrand,*[,§] and Gernot Frenking*[,†]

[†]Fachbereich Chemie, Philipps-Universität Marburg, Hans-Meerwein-Strasse, D-35032 Marburg, Germany

[‡]Institut für Anorganische Chemie, Georg-August-Universität, Tammannstrasse 4, 37077 Göttingen, Germany

[§]UCSD-CNRS Joint Research Chemistry Laboratory (UMI 3555), Department of Chemistry and Biochemistry, University of California−San Diego, La Jolla, California 92093-0343, United States

Supporting Information

ABSTRACT: Quantum chemical calculations using density functional theory have been carried out for the cyclic (alkyl)(amino)carbene (cAAC) complexes of the group 11 atoms [TM(cAAC)$_2$] (TM = Cu, Ag, Au) and their cations [TM(cAAC)$_2$]$^+$. The nature of the metal−ligand bonding was investigated with the charge and energy decomposition analysis EDA-NOCV. The calculations show that the TM−C bonds in the charged adducts [TM(cAAC)$_2$]$^+$ are significantly longer than in the neutral complexes [TM(cAAC)$_2$], but the cations have much higher bond dissociation energies than the neutral molecules. The intrinsic interaction energies ΔE_{int} in [TM(cAAC)$_2$]$^+$ take place between TM$^+$ in the ^{1}S electronic ground state and (cAAC)$_2$. In contrast, the metal−ligand interactions in [TM(cAAC)$_2$] involve the TM atoms in the excited ^{1}P state yielding strong TM p(π) → (cAAC)$_2$ π backdonation, which is absent in the cations. The calculations suggest that the cAAC ligands in [TM(cAAC)$_2$] are stronger π acceptors than σ donors. The trends of the intrinsic interaction energies and the bond dissociation energies of the metal−ligand bonds in [TM(cAAC)$_2$] and [TM(cAAC)$_2$]$^+$ give the order Au > Cu > Ag. Calculations at the nonrelativistic level give weaker TM−C bonds, particularly for the gold complexes. The trend for the bond strength in the neutral and charged adducts without relativistic effects becomes Cu > Ag > Au. The EDA-NOCV calculations suggest that the weaker bonds at the nonrelativistic level are mainly due to stronger Pauli repulsion and weaker orbital interactions. The NBO picture of the C−TM−C bonding situation does not correctly represent the nature of the metal−ligand interactions in [TM(cAAC)$_2$].

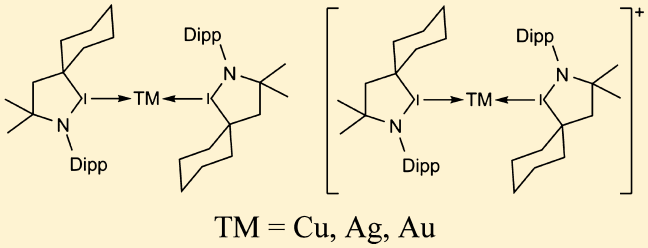

TM = Cu, Ag, Au

INTRODUCTION

The stabilization of small low-valent main-group elements by complexation with N-heterocyclic carbenes (NHCs) has been an area of intensive research in recent years.[1] Experimental studies reported about NHC stabilized molecular complexes of bare C,[2] Si,[3] and Ge[4] atoms in the singlet ^{1}D state and even the atomic dication Ge^{2+},[5] diatomic species Si_2,[6a] Ge_2,[6b] Sn_2,[6c] P_2,[7a,b] As_2,[7c] and B_2[8] as well as larger molecules such as $SiCl_2$,[9a] $GeCl_2$,[5,6b] and $SnCl_2$.[9b] An interesting variant of ligand stabilization of small species utilizes the particular properties of cyclic (alkyl)(amino)carbenes (cAACs),[10] which were found to stabilize BH in the unusual complex (BH)(cAAC)$_2$[11] as well as a wide variety of boron, carbon, silicon, and phosphorus based radicals.[12] A particular feature of the cAAC ligand is the ability to provide homoleptic dicoordinated complexes with transition metals such as manganese(0)[13] and zinc(0).[14] The bonding analysis of the latter complex Zn(cAAC)$_2$, which is a singlet biradical, showed that the zinc atom utilizes its vacant 4p orbitals for the donor−acceptor interaction with the carbene ligands.[14]

Chemical bonding of transition elements uses the s and d valence orbitals of the metals, while the p orbitals are much less important.[15] It has therefore been suggested that stable transition metal compounds possess 12 electrons in the valence shell rather than 18 electrons.[16a−d] Quantum chemical studies showed that the lowest lying empty p functions of transition metals have similar relevance as the valence s function, and therefore, they should be considered as genuine valence orbitals.[15a,17] This is the theoretical fundament of the 18 electron role for stable transition metal complexes,[15b,c] while the 8 electron role is valid for stable main group compounds that employ the valence s and p orbitals of the atoms for chemical bonding.[18] A reconciliation between the conflicting viewpoints of 12 or 18 valence electrons in transition metal bonding was provided by Pyykkö, who suggested that the p-like molecular orbitals with one nodal surface that are found in the complexes may have rather small contributions from the metal and that they are mainly localized at the ligands.[16e] This is in

Received: August 28, 2014
Published: November 13, 2014

   dx.doi.org/10.1021/ja508887s | J. Am. Chem. Soc. 2014, 136, 17123−17135

agreement with the bonding analysis of icosahedral compounds $[TM(ER)_{12}]$ (TM = Cr, Mo, W; E = Zn, Cd, Hg),[16f,g] which are model systems of recently isolated complexes that possess unusually high coordination numbers.[16g−j] Transition metal compounds exhibit sd + p bonding, while main group compounds feature sp bonding.

Very recently, we reported about the synthesis and structural characterization of the coinage metal complexes $[TM(cAAC)_2]$ (TM = Cu, Au), which possess a linear arrangement of the carbene ligands cAAC → TM ← cAAC and a doublet electronic state.[19,20] The group-11 atoms copper, silver and gold have a ^2S electronic ground state with the valence electron configuration $nd^{10}(n + 1)s^1(n + 1)p^0$. This poses the question about the location and the associated orbital of the unpaired electron and the nature of the vacant metal orbitals, which are involved in the cAAC → TM ← cAAC donor−acceptor interactions. In this paper, we report about the analysis of the bonding situation in the complexes $[TM(cAAC)_2]$ (Scheme 1)

Scheme 1. Schematic Representation of the Molecules That Are Studied in This Work

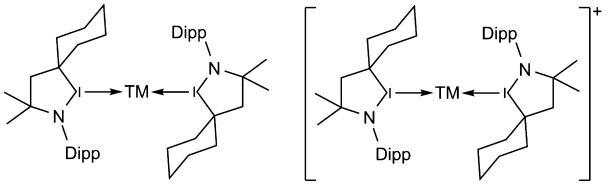

with the newly developed energy decomposition analysis in combination with the natural orbitals for chemical valence method (EDA-NOCV),[21] which is a powerful tool that provides detailed insights into the electronic structure.[22] The results are very surprising and provide new aspects for chemical bonding of the coinage metals. We also report about the structures and bonding of the related cations $[TM(cAAC)_2]^+$ (TM = Cu−Au), which are experimentally known for TM = Cu[20] and Au.[23] The calculated results for the silver complexes $[Ag(cAAC)_2]$ and $[Ag(cAAC)_2]^+$, which have not been isolated yet, may be helpful for future experiments.

METHODS

Geometry optimizations without symmetry constraints have been carried out with the Gaussian09 optimizer[24] using the DFT meta-hybrid functional M06[25] in conjunction with def2-SVP[26a] basis sets and a relativistic small-core pseudopotential for gold and silver.[26b] Stationary points were characterized as minima by calculating the Hessian matrix analytically at this level of theory.[27] The NBO[28] analyses have been carried out with the internal module of Gaussian09 at the M06/def2-SVP level of theory.

For the bonding analyses we calculated the molecules at the M06/def2-SVP optimized geometries with the program package ADF2013.01[29] using the DFT functional BP86[30] in conjunction with uncontracted Slater-type orbitals (STOs) as basis functions.[31] The latter basis sets for all elements have triple-ζ quality augmented by two sets of polarization functions. This level of theory is denoted BP86/TZ2P+. An auxiliary set of s, p, d, f, and g STOs was used to fit the molecular densities and to represent the Coulomb and exchange potentials accurately in each SCF cycle.[32] Scalar relativistic effects have been incorporated by applying the zeroth-order regular approximation (ZORA) in the ADF calculations.[33] The BP86/TZ2P+ calculations have been carried out using the frozen core approximation. All-electron calculations using BP86 were also performed in order to study the influence of the calculated energies. To this end we used TZP basis sets with and without applying the ZORA approximation, because nonrelativistic TZ2P+ basis sets are not available. The latter calculations are denoted as BP86/TZP(ZORA) and BP86/TZP(NR), respectively.

The interatomic interactions were investigated by means of an energy decomposition analysis (EDA, also known as extended transition state method, ETS) developed independently by Morokuma[34] and by Ziegler and Rauk.[35] The bonding analysis focuses on the instantaneous interaction energy ΔE_{int} of a bond A−B between two fragments A and B in the particular electronic reference state and in the frozen geometry of AB. This interaction energy is divided into three main components [eq 1].

$$\Delta E_{int} = \Delta E_{elstat} + \Delta E_{Pauli} + \Delta E_{orb} \quad (1)$$

The term ΔE_{elstat} corresponds to the quasiclassical electrostatic interaction between the unperturbed charge distributions of the prepared atoms and is usually attractive. The Pauli repulsion ΔE_{Pauli} is the energy change associated with the transformation from the superposition of the unperturbed electron densities $\rho_A + \rho_B$ of the isolated fragments to the wave function $\Psi^0 = N\hat{A}[\Psi_A\Psi_B]$, which properly obeys the Pauli principle through explicit antisymmetrization ($\hat{A}$ operator) and renormalization (N = constant) of the product wave function. ΔE_{Pauli} comprises the destabilizing interactions between electrons of the same spin on either fragment. The orbital interaction ΔE_{orb} accounts for charge transfer and polarization effects. The ΔE_{orb} term can be decomposed into contributions from each irreducible representation of the point group of the interacting system.

$$-D_e = \Delta E_{int} + \Delta E_{prep} \quad (2)$$

The difference between the interaction energy ΔE_{int} and the bond dissociation energy D_e is given by the relaxation of the fragments A and B from the electronic state and the geometry in the molecule to the equilibrium geometries and electronic ground states. This term is called preparation energy ΔE_{prep} [eq 2].[35] In case of the neutral complexes $[TM(cAAC)_2]$ there are contributions from the electronic excitation of TM atom from the $[(n - 1)d^{10}(n)s^1(n)p^0]$ ^2S ground state to the $[(n - 1)d^{10}(n)s^0(n)p^1]$ ^2P excited state and from the geometry changes of the ligands cAAC. In case of the cations $[TM(cAAC)_2]^+$ there are only contributions from the ligand relaxation, because the atomic ions TM^+ bind in their $[(n - 1)d^{10}(n)s^0(n)p^0]$ ^1S ground state. Further details on the EDA/ETS method[29] and its application to the analysis of the chemical bond[36] can be found in the literature.

The EDA-NOCV[37] method combines charge (NOCV) and energy (EDA) decomposition schemes to decompose the deformation density, which is associated with the bond formation, $\Delta\rho$, into different components of the chemical bond. The EDA-NOCV calculations provide pairwise energy contributions for each pair of interacting orbitals to the total bond energy. Natural orbital for chemical valence (NOCV)[38,39] is defined as the eigenvector of the valence operator, $\hat{V}$, given by eq 3:

$$\hat{V}\Psi_i = \upsilon_i\Psi_i \quad (3)$$

Here, the valence operator matrix is defined as $\hat{V} = 0.5\Delta P$ where ΔP corresponds to the difference between the charge- and bond-order matrices of the molecule and the promolecule which is the set of isolated atoms or molecular fragments. In the EDA-NOCV[37] scheme the orbital interaction term, ΔE_{orb}, is given by eq 4:

$$\Delta E_{orb} = \sum_k \Delta E_k^{orb} = \sum_{k=1}^{N/2} \nu_k[-F_{-k,-k}^{TS} + F_{k,k}^{TS}] \quad (4)$$

in which $F_{-k,-k}^{TS}$ and $F_{k,k}^{TS}$ are diagonal transition state Kohn−Sham matrix elements over the NOCVs φ_{-k} and φ_k with the eigenvalues $-\nu_k$ and ν_k, respectively, which arise from the diagonalization of the density matrix. For further details we refer to the original publication.[37] The ΔE_k^{orb} terms of a particular type of bond are assigned by visual inspection of the shape of the deformation density, $\Delta\rho_k$. The latter term is a measure of the size of the charge deformation and it provides a visual notion of the charge flow that is associated with the pairwise

dx.doi.org/10.1021/ja508887s | J. Am. Chem. Soc. 2014, 136, 17123−17135

orbital interaction. The EDA-NOCV scheme thus provides both qualitative ($\Delta\rho_{orb}$) and quantitative (ΔE_{orb}) information about the strength of pairwise orbital interactions in chemical bonds, even in molecules with C_1 symmetry.[22]

RESULTS AND DISCUSSION

The results of the work are divided in four sections. First, we present the results for the neutral complexes [TM(cAAC)$_2$]. Second, we discuss the data for the cations [TM(cAAC)$_2$]$^+$. In the third section we critically examine the NBO picture of the neutral and charged complex. The effect of relativistic contribution to the metal−ligand bonding is analyzed in the fourth section.

Neutral Complexes [TM(cAAC)$_2$]. The optimized geometries and the most important bond lengths and angles of the complexes [TM(cAAC)$_2$] (TM = Cu, Ag, Au) at M06/def2-SVP are shown in Figure 1. Experimental data of the copper and gold compounds are given in parentheses. The agreement between the calculated and the experimental values is quite good. The experimental data for the Cu−C and Au−C bond lengths are a bit smaller than the calculated results, which is likely due to intermolecular forces. It has been shown that solid-state interactions lead to a shortening of donor−acceptor bonds compared with gas-phase structures.[40] The angle C1-TM−C3 is in all complexes ∼180°, which indicates a nearly linear placement of the cAAC ligands at the metal atom. The nonplanar five-membered rings of the cAAC ligands are arranged in a coplanar fashion and a *trans*-arrangement of the nitrogen atoms as indicated by the calculated dihedral angles N1−C1−C3-N2, which deviate only slightly from 180°. The theoretical values are 190.4° for the copper complex, 190.2° for the silver complex and 189.0° for the gold complex.

Figure 1 shows also the calculated bond dissociation energies (BDEs) for the reactions [TM(cAAC)$_2$] → TM + 2 cAAC, which display the order Au > Cu > Ag. The bond strength raises the question about the nature of the metal−ligand interactions in the radicals. Important information about the metal−ligand bonding interactions comes from the shape of the singly occupied orbital of [TM(cAAC)$_2$], which is the energetically highest occupied molecular orbital (HOMO) of the complexes. Figure 2a shows the HOMO of [Cu(cAAC)$_2$], which is a delocalized three-center bonding π orbital of the C1−Cu−C3 moiety. The AO component at Cu is a p(π) orbital. It follows that the bonding interaction between copper and the carbene ligands involves the valence electron configuration $3d^{10}4s^04p^1$ of the excited ^{2}P state rather than the $3d^{10}4s^14p^0$ configuration of the ^{2}S ground state. The shape of the HOMO suggests that the singly occupied 4p AO of copper is strongly engaged in cAAC ← TM → cAAC π backdonation.

The electronic excitation 4s → 4p, which leads to the valence configuration $3d^{10}4s^04p^1$ at Cu, yields a vacant 4s AO at copper that may now serve as acceptor orbital for the in-phase (+,+) donation of the lone-pair electrons of the ligands. Figure 2b shows that the HOMO−1 exhibits the shape of this orbital, which is associated with the (+,+) cAAC → TM ← cAAC σ donation. The second lone-pair donation that arises through the out-of-phase (+,−) donation of the lone-pair electrons is nicely identified with the HOMO−2 (Figure 2c). It becomes obvious that the acceptor orbitals at Cu are the vacant 4s and 4p(σ) AOs, which have the right symmetry for the (+,+) and (+,−) orbital interactions. Figure 2b,c may be taken as textbook examples for the DCD (Dewar-Chatt-Duncanson)[41] model of

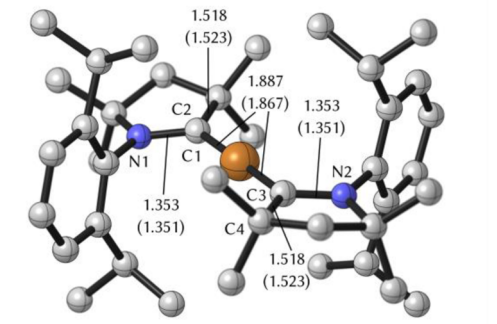

C2-C1-Cu: 130.2 (129.7) C4-C3-Cu: 130.2 (129.7)
N1-C1-Cu: 122.3 (123.0) N2-C3-Cu: 122.3 (123.0)
N1-C1-C2: 107.5 (107.3) N2-C3-C4: 107.5 (107.3)

(a) [Cu(cAAC)$_2$] (D_e = 91.2 kcal/mol)

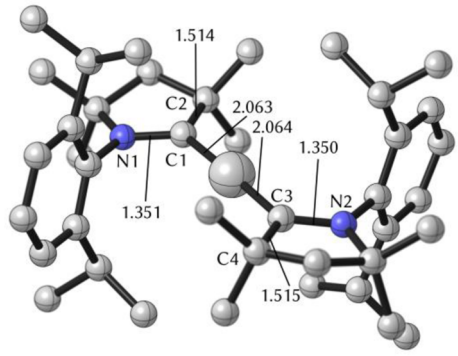

C2-C1-Ag: 128.2 C4-C3-Ag: 128.3
N1-C1-Ag: 123.1 N2-C3-Ag: 123.7
N1-C1-C2: 108.1 N2-C3-C4: 108.0

(b) [Ag(cAAC)$_2$] (D_e = 63.8 kcal/mol)

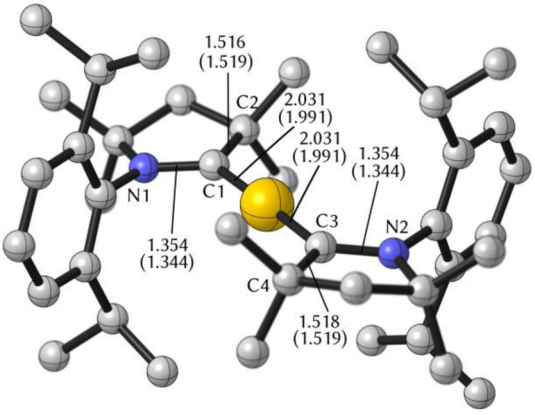

C2-C1-Au: 127.4 (126.2) C4-C3-Au: 127.1 (126.2)
N1-C1-Au: 124.2 (124.8) N2-C3-Au: 124.7 (124.8)
N1-C1-C2: 108.3 (108.9) N2-C3-C4: 108.2 (108.9)

(c) [Au(cAAC)$_2$] (D_e = 99.0 kcal/mol)

Figure 1. Optimized geometries of the neutral complexes [TM(cAAC)$_2$] at M06/def2-SVP. Calculated bond lengths in Å and angles in degree. Experimental values for the copper[20] and gold[19] complexes are given in parentheses. Calculated bond dissociation energies D_e for the fission of both TM−C bonds [TM(cAAC)$_2$] → TM + 2 cAAC at BP86/TZ2P+//M06/def2-SVP.

dx.doi.org/10.1021/ja508887s | J. Am. Chem. Soc. 2014, 136, 17123−17135

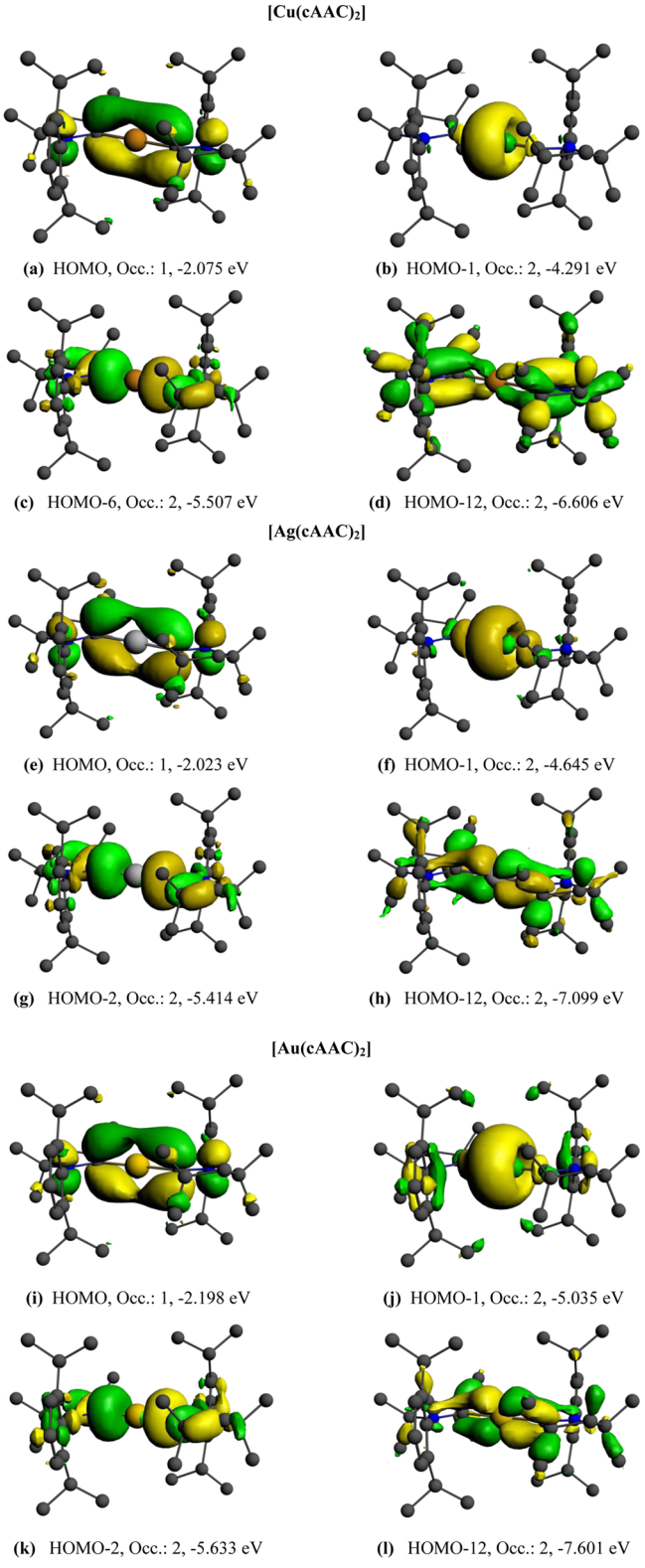

Figure 2. Plot of the occupied molecular orbitals of $[TM(cAAC)_2]$ at M06/def2-SVP that are relevant for the TM−C bonding.

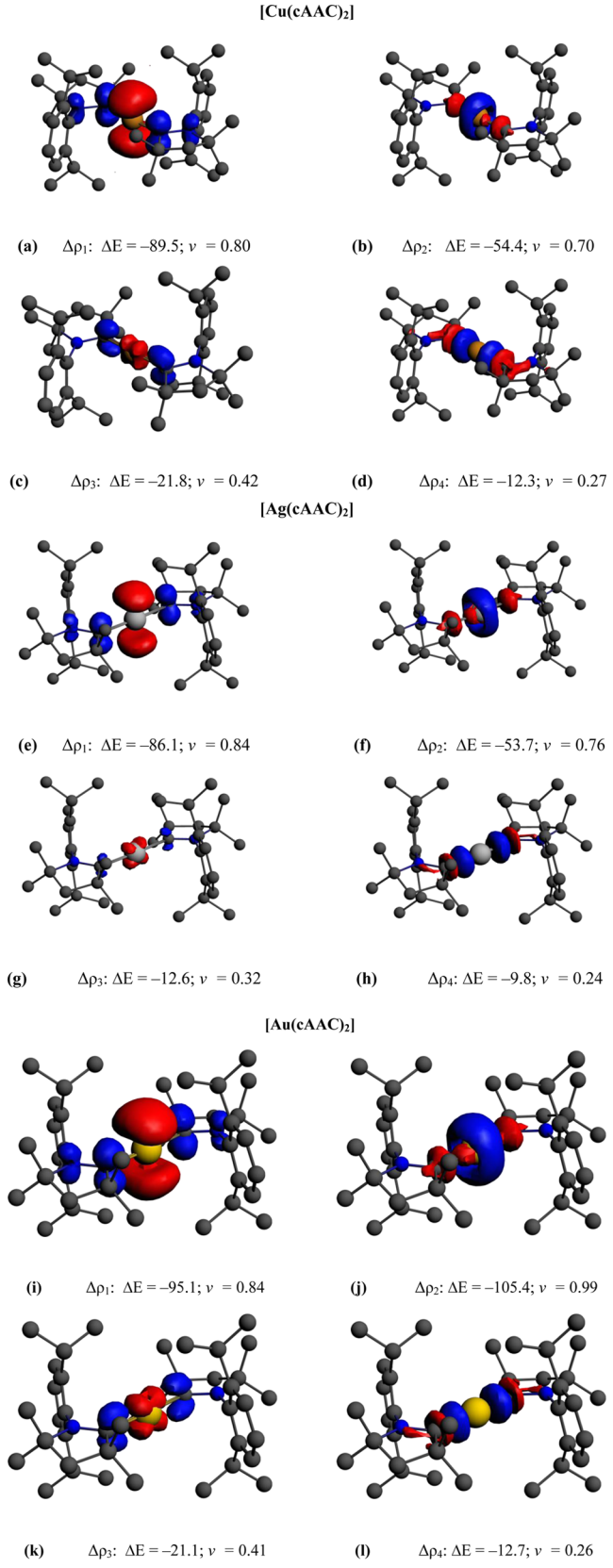

Figure 3. Deformation densities $\Delta\rho$ that are connected with the pairwise orbital interactions in $[TM(cAAC)_2]$ at BP86/TZ2P+ //M06/def2-SVP (Table 1). The charge flow of the electronic charge is red → blue. The associated orbital interaction energies ΔE are given in kcal/mol. The eigenvalues ν indicate the size of the charge flow.

L → TM ← L σ donation where the d_z2 AO is occupied, while Figure 3a depicts L ← TM → L π backdonation, which comes from a p(π) orbital of the metal. But where is the L ← TM → L π backdonation, which involves 3d(π) orbitals? We searched the orbitals and found that the HOMO−12 may be identified

dx.doi.org/10.1021/ja508887s | J. Am. Chem. Soc. 2014, 136, 17123−17135

with cAAC ← TM → cAAC π backdonation, which comes from the occupied $3d_{yz}$ AO of copper (Figure 2d).

Inspection of the molecular orbitals of $[Ag(cAAC)_2]$ and $[Au(cAAC)_2]$ reveals the same situation in the heavier homologues of the copper species. Figures 2e–h show the HOMO, HOMO−1, HOMO−2 and HOMO−12 of $[Ag(cAAC)_2]$, which closely resemble the analogous MOs of $[Cu(cAAC)_2]$. This holds also true for the orbitals of $[Au(cAAC)_2]$, which are displayed in Figure 2i–l. The shape of the orbitals suggests that the dominant orbital interaction in all complexes $[TM(cAAC)_2]$ comes from the σ donation of the ligands into the vacant (n)s and (n)p(σ) of TM, from the π backdonation of the singly occupied (n)p(π) AO, and from the doubly occupied $(n-1)d_{yz}$ AO of the metals. But what is the relative strength of the four orbital interactions? In order to answer this question, we carried out EDA-NOCV calculations of $[TM(cAAC)_2]$ using the naked metal atoms in the excited electron configuration TM ($d^{10}s^0p(\pi)^1$) and the ligands $(cAAC)_2$ as interacting fragments.[52] The results give a comprehensive picture of the nature of the metal–ligand interactions. The numerical values are shown in Table 1.

Table 1. EDA-NOCV Results of $[TM(cAAC)_2]$ at BP86/TZ2P+

		TM ($d^{10}s^0p(\pi)^1$) + $(cAAC)_2$[c]		
interacting fragments		$[Cu(cAAC)_2]$	$[Ag(cAAC)_2]$	$[Au(cAAC)_2]$
ΔE_{int}		−214.0	−177.8	−249.6
ΔE_{Pauli}		258.9	281.6	395.3
ΔE_{elstat}[a]		−273.5 (57.8%)	−277.9 (60.5%)	−381.8 (59.2%)
ΔE_{orb}[a]		−199.4 (42.2%)	−181.5 (39.5%)	−263.1 (40.8%)
$\Delta E_{orb,\sigma(1)}$[b]	TM (s) ← $(cAAC)_2$	−54.5 (27.3%)	−53.7 (29.6%)	−105.4 (40.1%)
$\Delta E_{orb,\sigma(2)}$[b]	TM p(σ) ← $(cAAC)_2$	−12.3 (6.1%)	−9.8 (5.4%)	−12.7 (4.8%)
$\Delta E_{orb,\pi(1)}$[b]	TM p(π) → $(cAAC)_2$	−89.5 (44.9%)	−86.1 (47.4%)	−95.1 (36.1%)
$\Delta E_{orb,\pi(2)}$[b]	TM d(π) → $(cAAC)_2$	−21.8 (10.9%)	−12.6 (6.9%)	−20.1 (7.6%)
$\Delta E_{orb,rest}$[b]		−21.3 (10.7%)	−19.3 (10.7%)	−39.8 (11.4%)
ΔE_{prep}		122.8	114.2	150.6
$\Delta E_{prep,TM}$		105.5	101.8	135.4
$-D_e$		−91.2	−63.6	−99.0

[a]The percentage values in parentheses give the contribution to the total attractive interactions $\Delta E_{elstat} + \Delta E_{orb}$. [b]The percentage values in parentheses give the contribution to the total orbital interactions ΔE_{orb}. [c]See reference 52.

The calculated interaction energies ΔE_{int} indicate that the strength of the intrinsic metal–ligand attraction has the trend Au > Cu > Ag. This is the general trend of the bond strength for transition metal complexes of the first, second, and third row of the d block atoms.[15b,c,42] Note that the bond dissociation energies D_e exhibit the same order Au > Cu > Ag but are much smaller than the intrinsic interaction energies ΔE_{int}, because the BDE considers the electronic and geometrical relaxation of the fragments. The preparation energies ΔE_{prep} that come mainly from the excitation energies of the metal atoms $^2S \rightarrow {}^2P$ are very large.

The breakdown of the ΔE_{int} values into the Pauli repulsion ΔE_{Pauli} and the two attractive components shows that roughly 60% comes from the electrostatic attraction ΔE_{elstat}, while ~40% comes from the orbital term ΔE_{orb}. The most interesting information is provided by the calculated strength of the four major pairwise orbital interactions that comprise ~90% of ΔE_{orb}. Table 1 shows that the dominant orbital interactions in $[Cu(cAAC)_2]$ and $[Ag(cAAC)_2]$ come from TM p(π) → $(cAAC)_2$ π backdonation followed by TM (s) ← $(cAAC)_2$ σ donation. The same result with reverse order is found for $[Au(cAAC)_2]$ where the latter term is a bit stronger than the former. The contributions of TM p(σ) ← $(cAAC)_2$ σ donation and TM d(π) → $(cAAC)_2$ π backdonation to ΔE_{orb} are in all complexes much smaller than the above terms.

The EDA-NOCV method makes it possible to visualize the charge flow that is associated with the pairwise orbital interactions. Figure 3 shows the deformation densities $\Delta\rho$, which are linked to the four most important orbital contributions. The color-coding gives the areas of charge depletion (red) and charge accumulation (blue) where the charge flow has the direction red → blue. Below each figure the calculated strength of the orbital interaction ΔE and the eigenvalue ν of the NOCV are given, which indicate the amount of charge that is displaced. Note that the eigenvalue ν and the associated energy value ΔE do not necessarily correlate!

Figure 3a shows the deformation density $\Delta\rho_1$, which is associated with the Cu(p_π) → $(cAAC)_2$ π backdonation that comes from the singly occupied orbital in $[Cu(cAAC)_2]$ into the formally empty p(π) orbitals of the carbene ligands, while Figure 3b exhibits the deformation density $\Delta\rho_2$, which comes from the Cu (s) ← $(cAAC)_2$ σ donation. The shape of $\Delta\rho_1$ nicely mirrors the size of the Cu p(π) → $(cAAC)_2$ π backdonation, which has a large eigenvalue of $\nu = 0.80$ and a stabilization energy of $\Delta E = -89.5$ kcal/mol, although only one electron is involved in the orbital interaction. The deformation density $\Delta\rho_2$ of the Cu (s) ← $(cAAC)_2$ σ donation has a smaller eigenvalue of $\nu = 0.70$ and $\Delta E = -54.4$ kcal/mol, although two electrons are involved in the donation. Figure 3c,d shows the charge flows that are associated with the weaker Cu d(π) → $(cAAC)_2$ π backdonation and Cu p(σ) ← $(cAAC)_2$ σ donation. The deformation densities $\Delta\rho$ that are connected to the most important pairwise orbital interactions in $[Ag(cAAC)_2]$ and $[Au(cAAC)_2]$ are shown in Figure 3e–l. The shape of the plots is very similar to the analogous charge flows of the copper complex.

The calculated eigenvalues ν of the most important deformation densities $\Delta\rho_1 - \Delta\rho_4$ suggest that the metal atoms in $[TM(cAAC)_2]$ serve mainly as electron donors rather than acceptors. This result is supported by the calculated partial charges, which are shown in Table 2. The coinage metals Cu, Ag, Au carry large positive charges q(TM) between 0.35 (Cu) and 0.51 (Ag) electrons, while the carbon atoms C1 and C3, which are bonded to the metal atoms and the cAAC ligands, are negatively charged. Thus, the cAAC ligands in $[TM(cAAC)_2]$

Table 2. Atomic Partial Charges q and Wiberg Bond Orders P of $[TM(cAAC)_2]$ at M06/def2-SVP

TM	Cu	Ag	Au
q(TM)	0.35	0.51	0.42
q(C1,C3)	−0.27	−0.13	−0.10
q(N1,N2)	−0.27	−0.52	−0.52
q(C2,C4)	−0.06	−0.12	−0.12
P(TM–C)	0.45	0.46	0.57

dx.doi.org/10.1021/ja508887s | J. Am. Chem. Soc. 2014, 136, 17123–17135

are stronger π acceptors than σ donors! The calculated partial charges[43] give the trend of the donor strength as Ag > Au > Cu. Note that the donor strength does not agree with the trend of the TM-$(cAAC)_2$ bond strength! This holds also for the calculated bond orders P(TM−C), which have the order Au > Ag > Cu. Bond orders and partial charges consider particular aspects of the electronic structure, but the overall strength of the interatomic interactions comes from several factors that are considered in the EDA-NOCV method.

The EDA-NOCV results that are shown in Table 1 and Figure 3 suggest that the most important valence orbitals of TM that are involved in the bonding with the cAAC ligands are the (n)s and (n)p orbitals, while the (n − 1)d orbitals are less important. The conclusion is that the coinage metals Cu, Ag, and Au bind in $[TM(cAAC)_2]$ complexes like main group elements.

Cations $[TM(cAAC)_2]^+$. Figure 4 shows the optimized geometries and the most important bond lengths and angles of the charged complexes $[TM(cAAC)_2]^+$ at M06/def2-SVP. The experimental values of the copper and gold compounds, which are given in parentheses, agree very well with the calculated data. The overall structures of the cations are very similar to the neutral species $[TM(cAAC)_2]$ (Figure 1). The metal atoms are always *trans*-coordinated by the cAAC ligands and the planes of the carbene ligands are for both systems arranged in a coplanar fashion where the nitrogen atoms are in a near *trans* position. The calculated dihedral angles N1−C1−C3-N2 in $[TM(cAAC)_2]^+$ deviate slightly more from 180° compared with the neutral complexes. The theoretical values are 192.3° for TM = Cu, 192.5° for TM = Ag, and 193.2° for TM = Au. The most important differences between the neutral and the charged species are found for the TM−C bond lengths, which are significantly longer in $[TM(cAAC)_2]^+$ than in $[TM(cAAC)_2]$. This holds for the theoretical values where the TM−C bonds in the cations are ∼0.05−0.06 Å longer than in the neutral complexes, while the experimental values of the cations are between 0.08 Å (Au−C) and 0.04 Å (Cu−C) longer. This is surprising given the fact that the metal cations TM^+ should bind the donor ligands stronger than the neutral atoms TM. The calculated BDEs of the charged complexes $[TM(cAAC)_2]^+$ are indeed much higher (D_e between 163.5−226.2 kcal/mol) than for the neutral systems $[TM(cAAC)_2]$. Both sets of BDEs possess the order Au > Cu > Ag. Stronger but longer bonds have been reported before,[44] but the differences that are exhibited here between the neutral and charged molecules are striking.

We analyzed the electronic structure of $[TM(cAAC)_2]^+$ with the goal to understand the bonding situation in the molecules. Since TM^+ has a $d^{10}s^0p^0$ (^1S) ground state, it can be expected that the donation of the in-phase (+,+) combination of the ligand lone-pair electrons into the vacant (n)s orbital of the metal TM(s) ← $(cAAC)_2$ should be a major component of the TM−C bonding. Inspection of the occupied orbitals of $[Cu(cAAC)_2]^+$ revealed three MOs (Figure 5a−c), which can be associated with Cu−C bonds. The HOMO of $[Cu(cAAC)_2]^+$ (Figure 5a) may be identified with Cu (s) ← $(cAAC)_2$ (+,+) σ donation. The HOMO−9 (Figure 5b) may likewise become assigned to the (+,−) σ donation into the vacant p(σ) AO Cu p(σ) ← $(cAAC)_2$. The search for metal d orbitals that are involved in the metal−ligand bonding led to the HOMO−11 (Figure 5c), which has a small coefficient at the d_{xz} AO that indicates some Cu d(π) → $(cAAC)_2$ π backdonation. But the shape of the orbitals does not reveal the

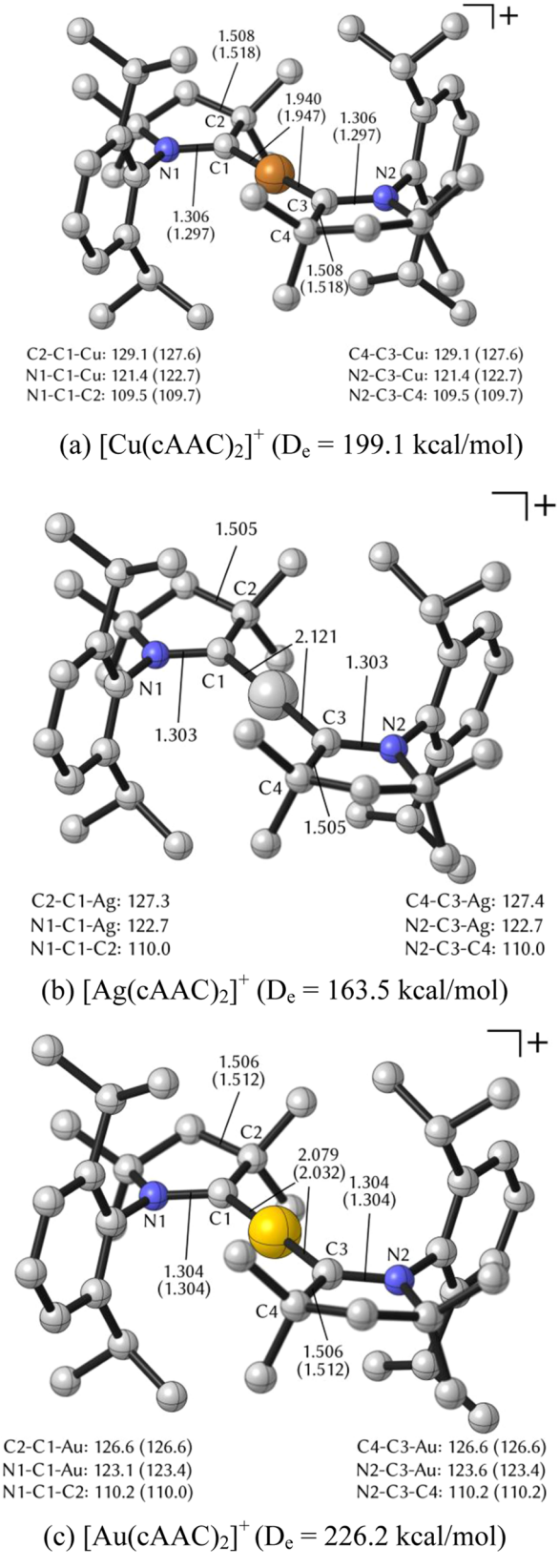

Figure 4. Optimized geometries of the charged complexes $[TM(cAAC)_2]^+$ at M06/def2-SVP. Calculated bond lengths in Å and angles in degrees. Experimental values for the copper[20] and gold[23] complexes are given in parentheses. Calculated bond dissociation energies D_e for fission of both TM−C bonds $[TM(cAAC)_2]^+ \rightarrow TM^+ + 2$ cAAC at BP86/TZ2P+//M06/def2-SVP.

dx.doi.org/10.1021/ja508887s | J. Am. Chem. Soc. 2014, 136, 17123−17135

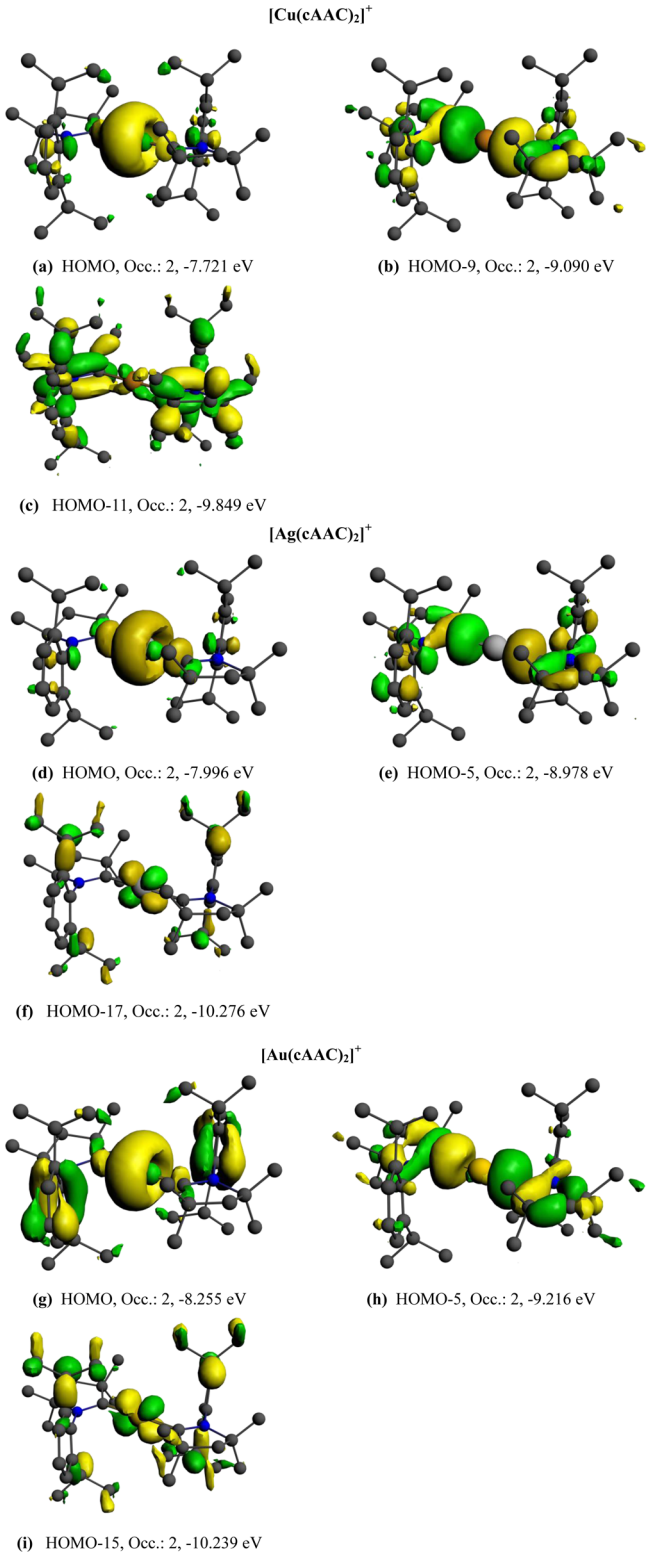

Figure 5. Plot of the occupied molecular orbitals of $[TM(cAAC)_2]^+$ at M06/def2-SVP that are relevant for the TM−C bonding.

strength of the interactions. Figure 5d−i shows the related occupied orbitals of the silver and gold homologues $[Ag(cAAC)_2]^+$ and $[Au(cAAC)_2]^+$, which have similar shapes as the orbitals of $[Cu(cAAC)_2]^+$. In order to specifically answer the question about the strength and nature of the metal−ligand interactions we turned to a more specific method.

We carried out EDA-NOCV calculations of $[TM(cAAC)_2]^+$ using TM^+ in the $d^{10}s^0p^0$ (^1S) ground state and $(cAAC)_2$ as interacting fragments. The numerical results are shown in Table 3. The preparation energies ΔE_{prep} are much smaller than for the neutral systems (Table 1) since the metal cation TM^+ is in the electronic ground state. The small ΔE_{prep} values come only from the geometrical relaxation of the ligands. The actual metal−ligand binding takes place between the promoted fragments, which means that the ΔE_{int} values rather than the D_e values must be used to estimate the strength of the interatomic interactions. Bond dissociation energies are not a good criterion for the strength of a chemical bond![45]

The calculated interaction energies nicely explain why the TM−C bonds in the neutral complexes are shorter than in the charged systems. A comparison of the EDA-NOCV results in Tables 1 and 3 show that the ΔE_{int} values of $[TM(cAAC)_2]$ are larger than those of $[TM(cAAC)_2]^+$. The crucial component that enhances the metal−ligand bonding in the neutral systems is the TM $p(\pi) \rightarrow (cAAC)_2$ π backdonation, which is absent in the cations. The EDA-NOCV calculations suggest that the TM $(s) \leftarrow (cAAC)_2$ σ donation, which is the largest component of ΔE_{orb} in $[TM(cAAC)_2]^+$ (Table 2), has nearly the same strength as in $[TM(cAAC)_2]$ (Table 1), while the TM $p(\sigma) \leftarrow (cAAC)_2$ σ donation in the cations is a bit stronger than in the neutral compounds. The TM $d(\pi) \rightarrow (cAAC)_2$ π backdonation in the cations is weaker than in the neutral system, which can be expected. There is also a contribution of TM $d(\sigma) \rightarrow (cAAC)_2$ σ backdonation in $[TM(cAAC)_2]^+$ (Table 2), which is usually not considered in the DCD bonding model. Note that the latter two terms have nearly the same strength.

The similar strength of the σ donation in the neutral and charged molecules can be related to the fact that the (n)s valence orbital of the metal is vacant in both systems. Nevertheless, it is a bit surprising that the TM $(s) \leftarrow (cAAC)_2$ σ donation in $[TM(cAAC)_2]^+$ is not much stronger than in $[TM(cAAC)_2]$, because the energy of the (n)s AO in TM^+ is much lower than in TM. On the other hand, the TM−C bonds in the neutral complexes are shorter than in the charged systems, which compensates for the difference between the energy levels of the (n)s acceptor orbitals in TM^+ and TM. But what is the reason for the shorter TM−C bonds in the neutral systems? Tables 1 and 3 show that the most important difference of the orbital interactions between $[TM(cAAC)_2]$ and $[TM(cAAC)_2]^+$ is the occurrence of strong TM $p(\pi) \rightarrow (cAAC)_2$ π backdonation in the neutral complexes. The additional π bonding induces significant bond shortening but only slightly stronger bonds in $[TM(cAAC)_2]$ since the (n)s acceptor orbital is energetically higher lying than in the cations.

Figure 6 shows the deformation densities $\Delta\rho$, which are associated with the orbital interactions. The deformation density $\Delta\rho_1$ (Figure 6a) nicely illustrates the Cu $(s) \leftarrow (cAAC)_2$ σ donation in $[Cu(cAAC)_2]^+$, which is the dominant term of ΔE_{orb} (Table 3). The deformation densities $\Delta\rho_2 - \Delta\rho_4$ (Figure 6b−d) display the charge flow that come from the Cu $p(\sigma) \leftarrow (cAAC)_2$ σ donation, $Cu(d_\pi) \rightarrow (cAAC)_2$ π backdonation and from the Cu $d(\sigma) \rightarrow (cAAC)_2$ σ backdonation. We want to point out that the deformation density $\Delta\rho_3$ has a larger eigenvalue (ν = 0.41) than $\Delta\rho_2$ (ν = 0.31), although the stabilization energy of the latter interaction is bigger (ΔE = −20.5 kcal/mol) than the former term (ΔE = −16.4 kcal/mol). Figure 6e−l displays the deformation densities of the silver and gold homologues $[Ag(cAAC)_2]^+$ and $[Au(cAAC)_2]^+$, which have similar shapes as [Cu-

dx.doi.org/10.1021/ja508887s | J. Am. Chem. Soc. 2014, 136, 17123−17135

Table 3. EDA-NOCV Results of $[TM(cAAC)_2]^+$ at BP86/TZ2P+

		TM^+ ($d^{10}s^0p^0$) + $(cAAC)_2$[c]		
interacting fragments		$[Cu(cAAC)_2]^+$	$[Ag(cAAC)_2]^+$	$[Au(cAAC)_2]^+$
ΔE_{int}		−211.5	−173.0	−237.1
ΔE_{Pauli}		190.0	216.2	319.4
ΔE_{elstat}[a]		−251.3 (62.6%)	−256.7 (66.0%)	−355.7 (63.9%)
ΔE_{orb}[a]		−150.2 (37.4%)	−132.5 (34.0%)	−200.8 (36.1%)
$\Delta E_{orb,\sigma(1)}$[b]	TM (s) ← $(cAAC)_2$	−53.5 (35.6%)	−54.1 (40.8%)	−101.4 (50.5%)
$\Delta E_{orb,\sigma(2)}$[b]	TM p(σ) ← $(cAAC)_2$	−20.5 (13.6%)	−16.1 (12.2%)	−19.9 (9.9%)
$\Delta E_{orb,\sigma(3)}$[b]	TM d(σ) → $(cAAC)_2$	−16.4 (10.9%)	−10.7 (8.1%)	−16.0 (8.0%)
$\Delta E_{orb,\pi(1)}$[b]	TM d(π) → $(cAAC)_2$	−14.7 (9.9%)	−10.4 (7.8%)	−15.6 (7.8%)
$\Delta E_{orb,rest}$[b]		−45.1 (30.0%)	−41.2 (31.1%)	−47.9 (23.8%)
ΔE_{prep}		12.4	9.5	10.9
$-D_e$		−199.1	−163.5	−226.2

[a]The percentage values in parentheses give the contribution to the total attractive interactions ΔE_{elstat} + ΔE_{orb}. [b]The percentage values in parentheses give the contribution to the total orbital interactions ΔE_{orb}. [c]See reference 552.

$(cAAC)_2]^+$. It becomes obvious that the Au (s) ← $(cAAC)_2$ σ donation is particularly strong. It is nearly twice as strong as in the copper and silver homologues, while the other terms have similar strengths for the three metal complexes $[TM(cAAC)_2]^+$.

The EDA-NOCV results indicate that the metal cations TM^+ in $[TM(cAAC)_2]^+$ are electron acceptors, which is not surprising. Table 4 shows the calculated partial charges of selected atoms, which suggest that the acceptor strength of TM^+ has the order Au > Ag > Cu. This is not the reverse order of the donor strength of TM in $[TM(cAAC)_2]$ (see above) and it does not follow the trend of the bond strength either. We want to point out that the partial charges at the metal atoms and at the carbon atoms of the TM−C bonds are both positive. A naive view would assume that the Coulomb interactions between the bonded atoms TM and carbon are repulsive. In contrast, the EDA-NOCV results in Table 3 indicate strong electrostatic attraction. Atomic partial charges are not a reliable indicator for electrostatic interactions, because they do not consider the spacial distribution of the electronic charge. Striking examples of this finding have been reported before.[15a,46]

It is interesting to compare the results of the cations $[TM(cAAC)_2]^+$ with the NHC homologues $[TM(NHC)_2]^+$, which are experimentally known for TM = Cu,[47a] Ag,[47a] Au.[47b,c] Structural data have been reported for $[Ag(NHC)_2]^+$[47a] and $[Au(NHC)_2]^+$[47b,c] but not for $[Cu(NHC)_2]^+$. The experimental values for the Au−C distances in $[Au(NHC^R)_2]^+$ where R = H (2.012 Å)[47b] and R = H, benzyl (2.026 Å)[47c] are very similar to the data for $[Au(cAAC)_2]^+$ (2.032 Å),[23] which has more bulky substituents at the carbene ligands. A theoretical study of $[TM(NHC)_2]^+$ with hydrogen at the nitrogen atoms gave slightly smaller TM−C bond dissociation energies at BP86/TZ2P of D_e = 194.8 kcal/mol (Cu), D_e = 154.3 kcal/mol (Ag) and D_e = 216.9 kcal/mol (Au).[48] It seems that the bonding situation in $[TM(NHC)_2]^+$ is not very different from $[TM(cAAC)_2]^+$.

NBO Picture of TM−C Bonds in $[TM(cAAC)_2]$ and $[TM(cAAC)_2]^+$. The bonding analysis of the complexes $[TM(cAAC)_2]$ revealed that the vacant p AOs of the transition metals play a very important role for the TM−C bonds. It is therefore interesting to find out the performance of the NBO method, because the p AOs of transition metals are not considered as genuine valence orbitals in the NBO procedure. The NBO method requires a preselection of the atomic basis functions in order to distinguish between valence orbitals that may become occupied in the population analysis and those orbitals that belong to the so-called Rydberg space that consists of the formally unoccupied orbitals.[28] The algorithm of the standard version of NBO uses a weighting factor that minimizes the contribution of the atomic (n)p functions of the transition metals to the bonding orbitals.[49] In a paper by Maseras and Morokuma[17a] it was shown that the (n)p population of the TMs changes significantly when a modified version of NBO with the valence space (n)s(n − 1)d(n)p is employed. Theoretical studies by Bayse and Hall[17b] and by Diefenbach et al.[15a] suggest that the (n)p AOs of transition metals are important for the chemical bonds, and therefore, they should be considered as genuine valence orbitals. In the light of the above finding it is interesting to see how the NBO method describes the metal−ligand bonding without using (n)p AOs of the metal.

Table 5 shows the results of NBO calculations for the TM−C bonds in $[TM(cAAC)_2]$ and $[TM(cAAC)_2]^+$. The most interesting data refer to the neutral systems where the (n)p AOs of the metal are particularly important. The bonding picture that is suggested by the NBO calculations for the C−TM−C moiety in $[TM(cAAC)_2]$ is schematically shown on top with the numerical data below the figure. The bonding situations in the three molecules are all different from each other. According to the NBO calculations, there is a single one-electron Cu−C bond between Cu and one cAAC ligand (occupation 0.97 e) that is strongly polarized toward carbon (87%). The bonded cAAC ligand still has a singly occupied "lone pair" orbital (occupation 0.86) at the carbon atom. The other cAAC ligand which has no bond to Cu possesses a lone-pair orbital at the carbon atom (occupation 1.92). Note that the calculated charge distribution of the NBO method gives an atomic charge of q = +0.35 for Cu (Table 2). The Wiberg bond order of the Cu−C bonds is P = 0.45. The latter values are in agreement with the EDA-NOCV calculations, which indicate that the TM p(π) → $(cAAC)_2$ backdonation is the most important part of the orbital interactions. This contribution to the bonding interactions is not recognized by the calculation of the bonding orbitals of the NBO method, because it is biased against mixing of (n)p functions for transition metals. Note that the bonding picture of the NBO analysis is not only in conflict with the EDA-NOCV calculations. It is also in conflict with the shape of the occupied valence orbitals of $[Cu(cAAC)_2]$, which are shown in Figure 2a−d.

dx.doi.org/10.1021/ja508887s | J. Am. Chem. Soc. 2014, 136, 17123−17135

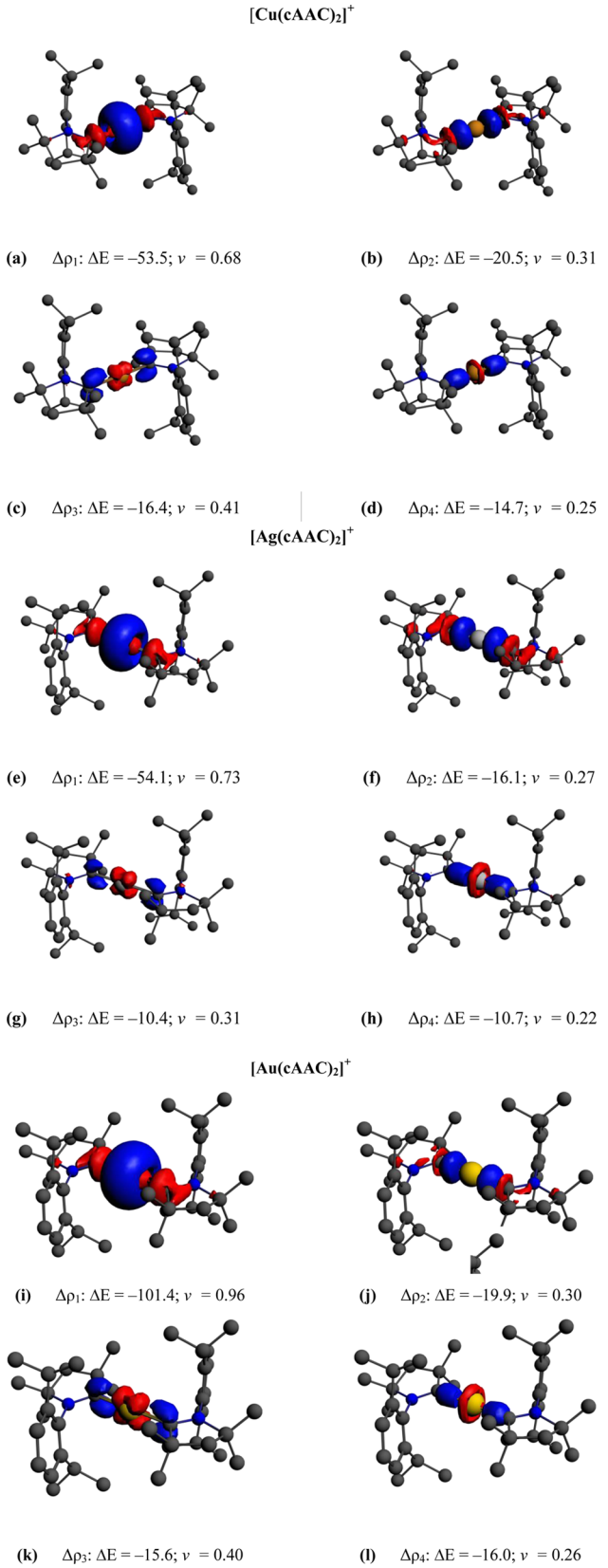

Figure 6. Deformation densities $\Delta\rho$ that are connected with the pairwise orbital interactions in $[TM(cAAC)_2]^+$ at BP86/TZ2P+ //M06/def2-SVP (Table 3). The charge flow of the electronic charge is red → blue. The associated orbital interaction energies ΔE are given in kcal/mol. The eigenvalues ν indicate the size of the charge flow.

Table 4. Atomic Partial Charges q and Wiberg Bond Orders P of $[TM(cAAC)_2]^+$ at M06/def2-SVP

TM	Cu	Ag	Au
q(TM)	0.68	0.55	0.42
q(C1,C3)	0.03	0.08	0.23
q(N1,N2)	−0.45	−0.45	−0.44
q(C2,C4)	−0.13	−0.13	−0.13
P(TM−C)	0.40	0.41	0.52

Table 5. NBO Results of the Bonding Situation in $[TM(cAAC)_2]$ and $[TM(cAAC)_2]^+$ at the M06/SVP Level of Theory[a]

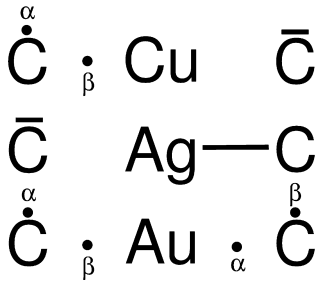

	TM−C bonds			
	occ.	polarization	hybridization (TM)	hybridization (C)
$Cu(cAAC)_2$	0.97	Cu: 13.1%, C: 86.9%	s (92.3%), d (7.7%)	s (38.2%), p (61.8%)
$Ag(cAAC)_2$	1.94	Ag: 16.4%, C: 83.6%	s (91.3%), d (8.7%)	s (35.9%), p (64.1%)
$Au(cAAC)_2$	0.98	Au: 22.6%, C: 77.4%	s (83.6%), d (17.3%)	s (35.6%), p (64.4%)
$Au(cAAC)_2$	0.98	Au: 23.2%, C: 76.8%	s (83.5%), d (16.3%)	s (35.7%), p (64.3%)
$[Cu(cAAC)_2]^+$	1.95	Cu: 12.6%, C: 87.5%	s (91.6%), d (8.2%)	s (34.9%), p (65.1%)
$[Ag(cAAC)_2]^+$	1.95	Ag: 14.8%, C: 85.2%	s (92.0%), d (7.9%)	s (33.1%), p (66.9%)
$[Au(cAAC)_2]^+$	1.96	Au: 21.9%, C: 78.1%	s (83.8%), d (16.1%)	s (33.0%), p (67.0%)
	carbene lone pairs			
	occ.	hybridization α		hybridization β
$Cu(cAAC)_2$ (LP1)	0.86	s (36.7%), p (63.3%)		–
$Cu(cAAC)_2$ (LP2)	1.92	s (36.7%), p (63.3%)		s (40.2%), p (59.8%)
$Ag(cAAC)_2$	1.68	s (34.5%), p (65.5%)		s (35.9%), p (64.1%)
$Au(cAAC)_2$ (LP1)	0.80	s (35.9%), p (64.1%)		–
$Au(cAAC)_2$ (LP2)	0.80	–		s (36.9%), p (63.2%)

[a]The picture shows schematically the bonding situation at the C−TM−C moiety in the neutral complexes as proposed by the NBO calculations.

The NBO results in Table 5 for the silver homologue $[Ag(cAAC)_2]$ give one doubly occupied TM−C bonding orbital (occupation 1.94) for one cAAC ligand, which is strongly polarized toward carbon (84%), while the other cAAC ligand is unbound and carries a lone-pair orbital (occupation 1.68). The hybridization of the Ag−C bond orbital reveals that it may be identified as a Ag (s) ← (cAAC) σ donor bond. There is no three-center C−Ag−C bonding orbital in $[Ag(cAAC)_2]$. Note that the polarization of the Ag−C bonding orbital does not agree with the shape of the HOMO−1 in the complex (Figure 2f), which has the largest extension at Ag.

The NBO results for bonding situation in the gold complex $[Au(cAAC)_2]$ suggest yet another scenario (Table 5). There

dx.doi.org/10.1021/ja508887s | J. Am. Chem. Soc. 2014, 136, 17123−17135

Table 6. EDA-NOCV Results of $[TM(cAAC)_2]$ with and without Relativistic Effects at BP86/TZP

		TM ($d^{10}s^0p(\pi)^1$) + $(cAAC)_2$[c]					
		relativistic (ZORA)			nonrelativistic		
interacting fragments		$[Cu(cAAC)_2]$	$[Ag(cAAC)_2]$	$[Au(cAAC)_2]$	$[Cu(cAAC)_2]$	$[Ag(cAAC)_2]$	$[Au(cAAC)_2]$
ΔE_{int}		−213.8	−176.0	−247.1	−204.1	−151.2	−146.9
ΔE_{Pauli}		261.9	281.3	395.3	261.3	293.5	427.5
ΔE_{elstat}[a]		−276.2 (58.1%)	−277.3 (60.6%)	−381.4 (59.4%)	−273.2 (58.7%)	−280.4 (63.1%)	−385.2 (67.1%)
ΔE_{orb}[a]		−199.5 (42.0%)	−180.0 (39.4%)	−261.0 (40.6%)	−192.2 (41.3%)	−164.3 (37.0%)	−189.2 (32.9%)
$\Delta E_{orb,\sigma(1)}$[b]	TM (s) ← $(cAAC)_2$	−54.7 (27.4%)	−53.4 (29.7%)	−105.1 (40.3%)	−49.0 (25.5%)	−43.7 (26.6%)	−58.4 (30.9%)
$\Delta E_{orb,\sigma(2)}$[b]	TM p(σ) ← $(cAAC)_2$	−12.1 (6.1%)	−9.2 (5.1%)	−13.4 (5.1%)	−11.6 (6.0%)	−8.3 (5.1%)	−9.7 (3.5%)
$\Delta E_{orb,\pi(1)}$[b]	TM p(π) → $(cAAC)_2$	−89.4 (44.8%)	−86.0 (47.8%)	−94.9 (36.4%)	−90.2 (46.9%)	−83.4 (50.8%)	−84.5 (44.7%)
$\Delta E_{orb,\pi(2)}$[b]	TM d(π) → $(cAAC)_2$	−22.0 (11.0%)	−12.6 (7.0%)	−20.0 (7.7%)	−21.0 (10.9%)	−11.3 (6.9%)	−15.1 (9.0%)
$\Delta E_{orb,rest}$[b]		−21.3 (10.7%)	−18.8 (10.4%)	−27.6 (10.6%)	−20.4 (10.6%)	−17.6 (10.7%)	−21.5 (11.4%)

[a]The percentage values in parentheses give the contribution to the total attractive interactions ΔE_{elstat} + ΔE_{orb}. [b]The percentage values in parentheses give the contribution to the total orbital interactions ΔE_{orb}. [c]See reference 52.

Table 7. EDA-NOCV Results of $[TM(cAAC)_2]^+$ with and without Relativistic Effects at BP86/TZP

		TM^+ ($d^{10}s^0p^0$) + $(cAAC)_2$[c]					
		relativistic (ZORA)			nonrelativistic		
interacting fragments		$[Cu(cAAC)_2]^+$	$[Ag(cAAC)_2]^+$	$[Au(cAAC)_2]^+$	$[Cu(cAAC)_2]^+$	$[Ag(cAAC)_2]^+$	$[Au(cAAC)_2]^+$
ΔE_{int}		−214.2	−171.9	−235.4	−203.4	−149.9	−142.9
ΔE_{Pauli}		195.0	215.7	318.8	197.5	223.9	348.1
ΔE_{elstat}[a]		−258.1 (63.1%)	−256.0 (66.1%)	−354.9 (64.1%)	−256.5 (64.0%)	−256.3 (68.5%)	−351.8 (71.6%)
ΔE_{orb}[a]		−151.2 (36.9%)	−131.6 (34.0%)	−199.2 (36.0%)	−144.4 (36.0%)	−117.6 (31.5%)	−139.2 (28.4%)
$\Delta E_{orb,\sigma(1)}$[b]	TM^+ (s) ← $(cAAC)_2$	−53.9 (35.6%)	−53.9 (41.0%)	−101.0 (50.7%)	−49.1 (34.0%)	−43.5 (37.0%)	−55.3 (39.7%)
$\Delta E_{orb,\sigma(2)}$[b]	TM^+ p(σ) ← $(cAAC)_2$	−20.4 (13.5%)	−15.5 (11.8%)	−19.1 (9.6%)	−19.7 (13.6%)	−14.2 (12.1%)	−14.7 (10.6%)
$\Delta E_{orb,\sigma(3)}$[b]	TM^+ d(π) → $(cAAC)_2$	−16.5 (10.9%)	−10.4 (7.9%)	−15.5 (7.8%)	−16.0 (11.1%)	−9.7 (8.2%)	−12.7 (9.1%)
$\Delta E_{orb,\pi(1)}$[b]	TM^+ d(π) → $(cAAC)_2$	−15.4 (10.2%)	−10.7 (8.1%)	−16.0 (8.0%)	−14.8 (10.2%)	−10.0 (8.5%)	−12.0 (8.6%)
$\Delta E_{orb,rest}$[b]		−45.0 (30.0%)	−41.1 (31.2%)	−47.6 (23.9%)	−44.8 (31.0%)	−40.2 (34.2%)	−44.5 (32.0%)

[a]The percentage values in parentheses give the contribution to the total attractive interactions ΔE_{elstat} + ΔE_{orb}. [b]The percentage values in parentheses give the contribution to the total orbital interactions ΔE_{orb}. [c]See reference 52.

are two one-electron Au−C bonds (occupation 0.98) and two singly occupied "lone-pair" orbitals at the cAAC ligands (occupation 0.80). According to the NBO picture, there are Au (s) ← (cAAC) σ donor bonds but no Au (s) → (cAAC) π back bonding. We searched the NBO orbitals for the excess unpaired electron and found that it is delocalized over the cAAC ligands.

Table 5 gives also the NBO bond orbitals for the cations $[TM(cAAC)_2]^+$. The calculations give one TM−C bond orbital, which is strongly polarized toward the cAAC ligand (between 78% for TM = Au and 88% for TM = Cu), while the other cAAC ligand is unbound. Somewhat surprisingly, the NBO calculations with different options do not give a three-center C−TM−C bond neither in the neutral systems nor in the cations, although the calculated atomic charges suggest a substantial charge donation cAAC → TM^+ ← cAAC, which is in agreement with the shape of the HOMO of the cations (Figure 5a,d,g).

We think that the deletion of the (n)p AOs of the coinage metals from the valence space creates problems for the NBO analysis of the bonding situation in the complexes $[TM(cAAC)_2]$.

Relativistic Effects. It is well-known that chemical bonding of heavy elements is strongly influenced by relativistic effects on the electronic structure of the atoms, which are particularly strong for gold.[50] The stronger bonds of gold compared with copper and silver are due to the relativistic effect on the atomic orbitals where the valence s and p orbitals are contracted, while the d and f orbitals are expanded. But also the lighter group-11 atoms silver and copper are subject to significant relativistic effects. Copper is the only atom of the first transition metal-row where relativistic effects have a profound influence on calculated bond lengths and bond energies.[50,51] It is very interesting to study the influence of relativity upon the EDA-NOCV results and to investigate the changes of the different terms that come from relativistic effects. Therefore, we carried out nonrelativistic EDA-NOCV calculations where the ZORA term is absent.

Table 6 gives the EDA-NOCV results with and without relativistic contribution for the neutral complexes $[TM(cAAC)_2]$. To this end we repeated the relativistic calculations using TZP all-electron basis sets and the ZORA method for the atoms, because nonrelativistic TZ2P+ basis sets are not available. A comparison with the relativistic data in Table 1, which have been obtained with the frozen core approximation and TZ2P+ basis sets show that the differences are very small. The nonrelativistic calculations at BP86/TZP(NR) (NR = nonrelativistic) in Table 6 reveal drastic changes particularly for the gold complex compared with the relativistic results at BP86/TZP(ZORA). The interaction energies at the nonrelativistic level are much smaller. The calculated ΔE_{int} values at BP86/TZP(NR) have the order Cu > Ag > Au, which follows the regular trend of the periodic system where heavier atoms of the same group have usually weaker bonds. The weakening of the interaction energy comes from the decrease of the orbital term ΔE_{orb}, while the electrostatic attraction ΔE_{elstat} changes

little and may even become slightly stronger without relativistic effects. Note that the weaker interaction energy for [Ag(cAAC)$_2$] and [Au(cAAC)$_2$] at the nonrelativistic level comes also from the stronger Pauli repulsion ΔE_{Pauli}, which increases particularly for the gold complex.

Inspection of the dominant orbital interactions shows that the smaller ΔE_{orb} term comes mainly from the decrease of the TM (s) ← (cAAC)$_2$ σ donation at the nonrelativistic level. The contribution of the latter term in [Au(cAAC)$_2$] is only −58.4 kcal/mol, which is reduced by nearly one-half of the relativistic value of −105.1 kcal/mol (Table 6). The other three major orbital contributions in [Au(cAAC)$_2$] are also weaker at the nonrelatistic level but the decrease is much less than for the Au (s) ← (cAAC)$_2$ σ donation. The latter interaction is the dominant orbital term at BP86/TZP(ZORA) but it becomes weaker than the Au p(π) → (cAAC)$_2$ π backdonation at BP86/TZP(NR). The largest changes of the four major orbital terms in [Cu(cAAC)$_2$] and [Ag(cAAC)$_2$] are also found for the TM (s) ← (cAAC)$_2$ σ donation but the weakening is much less than in [Au(cAAC)$_2$].

Table 7 shows the EDA-NOCV results with and without relativistic contributions for the charged complexes [TM(cAAC)$_2$]$^+$. The change of the calculated data from BP86/TZP(ZORA) to BP86/TZP(NR) is similar to the changings that are found for the neutral species. The largest variation is observed for the gold complex. The total interaction energy at the nonrelativistic level has the order Cu > Ag > Au. The smaller ΔE_{int} values at BP86/TZP(NR) are mainly due to the stronger Pauli repulsion and from the weaker orbital interaction. The weakening of the ΔE_{orb} term is primarily due to the much smaller TM (s) ← (cAAC)$_2$ σ donation at the nonrelativistic level.

SUMMARY AND CONCLUSION

The results of this work can be summarized as follows. The calculated geometries of the neutral and charged complexes [TM(cAAC)$_2$] and [TM(cAAC)$_2$]$^+$ (TM = Cu, Ag, Au) at M06/SVP are in very good agreement with the experimental values of the copper and gold species. The calculations show that the TM−C bonds in the charged adducts [TM(cAAC)$_2$]$^+$ are significantly longer than in the neutral complexes [TM(cAAC)$_2$] but the cations have much higher bond dissociation energies than the neutral molecules. This finding is explained with the nature of the metal−ligand interactions, which are analyzed with the help of EDA-NOCV calculations. The metal−ligand interactions in [TM(cAAC)$_2$] involve the TM atoms in the excited ^{1}P state where the unpaired electron is in the (n)p orbital. This leads to a strong TM p(π) → (cAAC)$_2$ π backdonation that is absent in the cations. The TM p(π) → (cAAC)$_2$ π backdonation is clearly the dominant term for the orbital interactions in [Cu(cAAC)$_2$] and [Ag(cAAC)$_2$] followed by TM (s) ← (cAAC)$_2$ σ donation. The TM p(π) → (cAAC)$_2$ π backdonation is a bit weaker than the TM (s) ← (cAAC)$_2$ σ donation in the gold complex [Au(cAAC)$_2$] but the overall contributions of the TM → (cAAC)$_2$ π backdonation to the orbital interactions are in all complexes larger than the TM ← (cAAC)$_2$ σ donation. This is supported by the calculated charge distribution, which gives positive charges for the metal atoms. The calculations suggest that the cAAC ligands in [TM(cAAC)$_2$] are stronger π acceptors than σ donors. The NBO picture of the C−TM−C bonding situation does not correctly represent the nature of the metal−ligand interactions in [TM(cAAC)$_2$].

The intrinsic interaction energies ΔE_{int} in [TM(cAAC)$_2$] between TM in the excited ^{2}P state and the ligands (cAAC)$_2$ are stronger than the metal−ligand interactions in the cations [TM(cAAC)$_2$]$^+$ that take place between TM$^+$ in the ^{1}S electronic ground state and (cAAC)$_2$. The bond dissociation energies of the neutral adducts [TM(cAAC)$_2$] are much smaller than the data for [TM(cAAC)$_2$]$^+$, because they consider the electronic relaxation of the TM atoms to the ground state.

The trend of the intrinsic interaction energies and the bond dissociation energies of the metal−ligand bonds in [TM(cAAC)$_2$] and [TM(cAAC)$_2$]$^+$ give the order Au > Cu > Ag. Calculations at the nonrelativistic level give weaker TM−C bonds, particularly for the gold complexes. The trend for the bond strength in the neutral and charged adducts without relativistic effects becomes Cu > Ag > Au. The EDA-NOCV calculations suggest that the weaker bonds at the nonrelativistic level are mainly due to stronger Pauli repulsion and weaker orbital interactions. The decline of the latter term comes mainly from the TM (s) ← (cAAC)$_2$ σ donation, which become clearly weaker when relativistic effects are not considered. Relativistic effects are also important for the copper complexes where the interaction energies are ∼10 kcal/mol smaller at the nonrelativistic level.

ASSOCIATED CONTENT

Supporting Information

Tables with the coordinates and energies of the calculated molecules. This material is available free of charge via the Internet at http://pubs.acs.org.

AUTHOR INFORMATION

Corresponding Authors

hroesky@gwdg.de
gbertrand@ucsd.edu
frenking@chemie.uni-marburg.de

Notes

The authors declare no competing financial interest.

ACKNOWLEDGMENTS

We are grateful to the referees for their thoughtful and constructive comments that helped to improve the paper. This work was supported by the Deutsche Forschungsgemeinschaft and the DOE (DE-FG02-13ER16370). Excellent service by the Hochschulrechenzentrum of the Philipps-Universität Marburg is gratefully acknowledged.

REFERENCES

(1) (a) Kuhn, N.; Al-Sheikh, A. *Coord. Chem. Rev.* **2005**, *249*, 829. (b) Wilson, D. J. D.; Dutton, J. L. *Chem.—Eur. J.* **2013**, *19*, 13626.

(2) (a) Dyker, C. A.; Lavallo, V.; Donnadieu, B.; Bertrand, G. *Angew. Chem., Int. Ed.* **2008**, *47*, 3206. (b) Fürstner, A.; Alcarazo, M.; Goddard, R.; Lehmann, C. W. *Angew. Chem., Int. Ed.* **2008**, *47*, 3210. (c) Lavallo, V.; Dyker, C. A.; Donnadieu, B.; Bertrand, G. *Angew. Chem., Int. Ed.* **2008**, *47*, 5411. (d) Alcarazo, M.; Lehmann, C. W.; Anoop, A.; Thiel, W.; Fürstner, A. *Nat. Chem.* **2009**, *1*, 295. (e) Melaimi, M.; Parameswaran, P.; Donnadieu, B.; Frenking, G.; Bertrand, G. *Angew. Chem., Int. Ed.* **2009**, *48*, 4792. (f) Fernandez, I.; Dyker, C. A.; DeHope, A.; Donnadieu, B.; Frenking, G.; Bertrand, G. *J. Am. Chem. Soc.* **2009**, *131*, 11875. (g) Melaimi, M.; Soleilhavoup, M.; Bertrand, G. *Angew. Chem., Int. Ed.* **2010**, *49*, 8810. (h) Inés, B.; Patil, M.; Carreras, J.; Goddard, R.; Thiel, W.; Alcarazo, M. *Angew. Chem., Int. Ed.* **2011**, *50*, 8400.

(3) (a) Mondal, K. C.; Roesky, H. W.; Klinke, F.; Schwarzer, M. C.; Frenking, G.; Niepötter, B.; Wolf, H.; Herbst-Irmer, R.; Stalke, D.

Angew. Chem., Int. Ed. **2013**, *52*, 2963. (b) Xiong, Y.; Yao, S.; Inoue, S.; Epping, J. D.; Driess, M. *Angew. Chem., Int. Ed.* **2013**, *52*, 7147.
(4) (a) Xiong, Y.; Yao, S.; Tan, G.; Inoue, S.; Driess, M. *J. Am. Chem. Soc.* **2013**, *135*, 5004. (b) Li, Y.; Mondal, K. C.; Roesky, H. W.; Zhu, H.; Stollberg, P.; Herbst-Irmer, R.; Stalke, D.; Andrade, D. M. *J. Am. Chem. Soc.* **2013**, *135*, 12422. (c) Chu, T.; Belding, L.; van der Est, A.; Dudding, T.; Korobkov, I.; Nikonov, G. I. *Angew. Chem., Int. Ed.* **2014**, *53*, 2711.
(5) Rupar, P. A.; Staroverov, V. N.; Ragogna, P. J.; Baines, K. M. *J. Am. Chem. Soc.* **2007**, *129*, 15138.
(6) (a) Wang, Y.; Xie, Y.; Wei, P.; King, R. B.; Schaefer, H. F., III; Schleyer, P. v. R.; Robinson, G. H. *Science* **2008**, *321*, 1069. (b) Sidiropoulos, A.; Jones, C.; Stasch, A.; Klein, S.; Frenking, G. *Angew. Chem., Int. Ed.* **2009**, *48*, 9701; *Angew. Chem.* **2009**, *121*, 9881. (c) Jones, C.; Sidiropoulos, A.; Holzmann, N.; Frenking, G.; Stasch, A. *J. Chem. Soc., Chem. Commun.* **2012**, *48*, 9855.
(7) (a) Wang, Y.; Xie, Y.; Wie, P.; King, R. B.; Schaefer, H. F., III; Schleyer, P. v. R.; Robinson, G. *J. Am. Chem. Soc.* **2008**, *130*, 14970. (b) Back, O.; Donnadieu, B.; Parameswaran, P.; Frenking, G.; Bertrand, G. *Nat. Chem.* **2010**, *2*, 369. (c) Abraham, M. Y.; Wang, Y.; Xie, Y.; Wei, P.; Schaefer, H. F., III; Schleyer, P. v. R.; Robinson, G. H. *Chem.—Eur. J.* **2010**, *16*, 432.
(8) Brauschweig, H.; Dewhurst, R. D.; Hammond, K.; Mies, J.; Radacki, K.; Vargas, A. *Science* **2012**, *336*, 1420.
(9) (a) Ghadwal, R. S.; Roesky, H. W.; Merkel, S.; Henn, J.; Stalke, D. *Angew. Chem., Int. Ed.* **2009**, *48*, 5683. (b) Kuhn, N.; Kratz, Th.; Bläser, D.; Boese, R. *Chem. Ber.* **1995**, *128*, 245.
(10) (a) Lavallo, V.; Canac, Y.; Präsang, C.; Donnadieu, B.; Bertrand, G. *Angew. Chem., Int. Ed.* **2005**, *44*, 5705. (b) Jazzar, R.; Dewhurst, R. D.; Bourg, J.-B.; Donnadieu, B.; Canac, Y.; Bertrand, G. *Angew. Chem., Int. Ed.* **2007**, *46*, 2899. (c) Melaimi, M.; Soleilhavoup, M.; Bertrand, G. *Angew. Chem., Int. Ed.* **2010**, *49*, 8810. (d) Martin, D.; Melaimi, M.; Soleilhavoup, M.; Bertrand, G. *Organometallics* **2011**, *30*, 5304.
(11) Kinjo, R.; Donnadieu, B.; Celik, M. A.; Frenking, G.; Bertrand, G. *Science* **2011**, *333*, 610.
(12) (a) Back, O.; Kuchenbeiser, G.; Donnadieu, B.; Bertrand, G. *Angew. Chem., Int. Ed.* **2009**, *48*, 5530. (b) Ruiz, D. A.; Ung, G.; Melaimi, M.; Bertrand, G. *Angew. Chem., Int. Ed.* **2013**, *52*, 7590. (c) Martin, C. D.; Weinstein, C. M.; Moore, C. E.; Rheingold, A. L.; Bertrand, G. *Chem. Commun.* **2013**, *49*, 4486. (d) Martin, C. D.; Soleilhavoup, M.; Bertrand, G. *Chem. Sci.* **2013**, *4*, 3020. (e) Mahoney, J. K.; Martin, D.; Moore, C. E.; Rheingold, A. L.; Bertrand, G. *J. Am. Chem. Soc.* **2013**, *135*, 18766. (f) Back, O.; Celik, M. A.; Frenking, G.; Melaimi, M.; Donnadieu, B.; Bertrand, G. *J. Am. Chem. Soc.* **2010**, *132*, 10262−10263. (g) Mondal, K. C.; Roesky, H. W.; Schwarzer, M. C.; Frenking, G.; Niepötter, B.; Wolf, H.; Herbst-Irmer, R.; Stalke, D. *Angew. Chem., Int. Ed.* **2013**, *52*, 2963. (h) Mondal, K. C.; Samuel, P. P.; Tretiakov, M.; Singh, A. P.; Roesky, H. W.; Stückl, A. C.; Niepötter, B.; Carl, E.; Wolf, H.; Herbst-Irmer, R.; Stalke, D. *Inorg. Chem.* **2013**, *52*, 4736.
(13) Samuel, P. P.; Mondal, K. C.; Roesky, H. W.; Hermann, M.; Frenking, G.; Demeshko, S.; Meyer, F.; Stückl, A. C.; Christian, J. H.; Dalal, N. S.; Ungur, L.; Chibotaru, L. F.; Pröpper, K.; Meents, A.; Dittrich, B. *Angew. Chem., Int. Ed.* **2013**, *52*, 11817.
(14) Singh, A. P.; Samuel, P. P.; Roesky, H. W.; Schwarzer, M. C.; Frenking, G.; Sidhu, N. S.; Dittrich, B. *J. Am. Chem. Soc.* **2013**, *135*, 7324.
(15) (a) Diefenbach, A.; Bickelhaupt, F. M.; Frenking, G. *J. Am. Chem. Soc.* **2000**, *122*, 6449. (b) Frenking, G.; Fröhlich, N. *Chem. Rev.* **2000**, *100*, 717. (c) Frenking, G. In *The Chemical Bond. Chemical Bonding Across the Periodic Table*; Frenking, G., Shaik, S., Eds.; Wiley-VCH: Weinheim, 2014; pp 175−218.
(16) (a) Landis, C. R.; Cleveland, T.; Firman, T. K. *J. Am. Chem. Soc.* **1995**, *117*, 1859. (b) Landis, C. R.; Firman, T. K.; Root, D. M.; Cleveland, T. *J. Am. Chem. Soc.* **1998**, *120*, 1842. (c) Landis, C. R.; Cleveland, T.; Firman, T. K. *J. Am. Chem. Soc.* **1998**, *120*, 2641. (d) Firman, T. K.; Landis, C. R. *J. Am. Chem. Soc.* **1998**, *120*, 12650. (e) Pyykkö, P. *J. Organomet. Chem.* **2006**, *691*, 4336. (f) Von Hopffgarten, M.; Frenking, G. *J. Phys. Chem. A* **2011**, *115*, 12758. (g) Cadenbach, T.; Bollermann, T.; Gemel, C.; Fernández, I.; von Hopffgarten, M.; Frenking, G.; Fischer, R. A. *Angew. Chem., Int. Ed.* **2008**, *47*, 9150. (h) Cadenbach, T.; Bollermann, T.; Gemel, C.; Tombul, M.; Fernandez, I.; von Hopffgarten, M.; Frenking, G.; Fischer, R. A. *J. Am. Chem. Soc.* **2009**, *131*, 16063. (i) Gonzalez-Gallardo, S.; Prabusankar, G.; Cadenbach, T.; Gemel, C.; von Hopffgarten, M.; Frenking, G.; Fischer, R. A. *Struct. Bonding (Berlin, Ger.)* **2010**, *136*, 147. (j) Bollermann, T.; Cadenbach, T.; Gemel, C.; von Hopffgarten, M.; Frenking, G.; Fischer, R. A. *Chem.—Eur. J.* **2010**, *16*, 13372.
(17) (a) Maseras, F.; Morokuma, K. *Chem. Phys. Lett.* **1992**, *195*, 500. (b) Bayse, C. A.; Hall, M. B. *J. Am. Chem. Soc.* **1999**, *121*, 1348.
(18) Kaupp, M. In *The Chemical Bond. Chemical Bonding Across the Periodic Table*; Frenking, G., Shaik, S., Eds.; Wiley-VCH: Weinheim, 2014; pp 1−24.
(19) TM = Au: Weinberger, D.; Melaimi, M.; Moore, C. E.; Rheingold, A. L.; Frenking, G.; Jerabek, P.; Bertrand, G. *Angew. Chem., Int. Ed.* **2013**, *52*, 8964.
(20) TM = Cu: Weinberger, D. S.; SK, N. A.; Mondal, K. C.; Melaimi, M.; Bertrand, G.; Stückl, A. C.; Roesky, H. W.; Dittrich, B.; Demeshko, S.; Schwederski, B.; Kaim, W.; Jerabek, P.; Frenking, G. *J. Am. Chem. Soc.* **2014**, *136*, 6235.
(21) Mitoraj, M. P.; Michalak, A.; Ziegler, T. *J. Chem. Theory Comput.* **2009**, *5*, 962.
(22) For recent examples see: (a) Devarajan, D.; Frenking, G. *Chem.—Asian J.* **2012**, *7*, 1296. (b) Nguyen, T. A. N.; Frenking, G. *Chem.—Eur. J.* **2012**, *18*, 12733. (c) Holzmann, N.; Dange, D.; Jones, C.; Frenking, G. *Angew. Chem., Int. Ed.* **2013**, *52*, 3004. (d) Mousavi, M.; Frenking, G. *Organometallics* **2013**, *32*, 1743. (e) Das, A.; Dash, C.; Celik, M. A.; Yousufuddin, M.; Frenking, G.; Dias, H. V. R. *Organometallics* **2013**, *32*, 3135. (f) Celik, M. A.; Frenking, G.; Neumüller, B.; Petz, W. *ChemPlusChem* **2013**, *78*, 1024. (g) Nguyen, T. A. N.; Frenking, G. *Mol. Phys.* **2013**, *111*, 2640. (h) Hermann, M.; Goedecke, C.; Jones, C.; Frenking, G. *Organometallics* **2013**, *32*, 6666. (i) Mondal, K. C.; Samuel, P. P.; Roesky, H. W.; Carl, E.; Herbst-Irmer, R.; Stalke, D.; Schwederski, B.; Kaim, W.; Ungur, L.; Chibotaru, L. F.; Hermann, M.; Frenking, G. *J. Am. Chem. Soc.* **2014**, *136*, 1770. (j) Caramori, G. F.; Garcia, L. C.; Andrada, D. M.; Frenking, G. *Organometallics* **2014**, *33*, 2301. (k) Holzmann, N.; Frenking, G. *Z. Naturforsch., A: Phys. Sci.* **2014**, *69*, 385.
(23) Frey, G. D.; Dewhurst, R. D.; Kousar, S.; Donnadieu, B.; Bertrand, G. *J. Organomet. Chem.* **2008**, *693*, 1674.
(24) Frisch, M. J.; Trucks, G. W.; Schlegel, H. B.; Scuseria, G. E.; Robb, M. A.; Cheeseman, J. R.; Scalmani, G.; Barone, V.; Mennucci, B.; Petersson, G. A.; Nakatsuji, H.; Caricato, M.; Li, X.; Hratchian, H. P.; Izmaylov, A. F.; Bloino, J.; Zheng, G.; Sonnenberg, J. L.; Hada, M.; Ehara, M.; Toyota, K.; Fukuda, R.; Hasegawa, J.; Ishida, M.; Nakajima, T.; Honda, Y.; Kitao, O.; Nakai, H.; Vreven, T.; Montgomery, J. A., Jr.; Peralta, J. E.; Ogliaro, F.; Bearpark, M.; Heyd, J. J.; Brothers, E.; Kudin, K. N.; Staroverov, V. N.; Kobayashi, R.; Normand, J.; Raghavachari, K.; Rendell, A.; Burant, J. C.; Iyengar, S. S.; Tomasi, J.; Cossi, M.; Rega, N.; Millam, N. J.; Klene, M.; Knox, J. E.; Cross, J. B.; Bakken, V.; Adamo, C.; Jaramillo, J.; Gomperts, R.; Stratmann, R. E.; Yazyev, O.; Austin, A. J.; Cammi, R.; Pomelli, C.; Ochterski, J. W.; Martin, R. L.; Morokuma, K.; Zakrzewski, V. G.; Voth, G. A.; Salvador, P.; Dannenberg, J. J.; Dapprich, S.; Daniels, A. D.; Farkas, O.; Foresman, J. B.; Ortiz, J. V.; Cioslowski, J.; Fox, D. J. *Gaussian 09*, Rev. C.01; Gaussian, Inc.: Wallingford, CT, 2010.
(25) Zhao, Y.; Truhlar, D. G. *Theor. Chem. Acc.* **2008**, *120*, 215.
(26) (a) Schaefer, A.; Horn, H.; Ahlrichs, R. *J. Chem. Phys.* **1992**, *97*, 2571. (b) Andrae, D.; Haeussermann, U.; Dolg, M.; Stoll, H.; Preuss, H. *Theor. Chim. Acta* **1990**, *77*, 123.
(27) Deglmann, P.; Furche, F.; Ahlrichs, R. *Chem. Phys. Lett.* **2002**, *362*, 511.
(28) (a) Landis, C. R.; Weinhold, F. *The Chemical Bond. 1. Fundamental Aspects of Chemical Bonding*; Frenking, G., Shaik, S., Eds.; Wiley-VCH: Weinheim, 2014; pp 91−120. (b) Landis, C. R.; Weinhold, F. *Valency and Bonding: A Natural Bond Orbital Donor-Acceptor Perspective*; Cambridge University Press: Cambridge, 2005.

(c) Landis Reed, A. E.; Curtiss, L. A.; Weinhold, F. *Chem. Rev.* **1988**, *88*, 899.
(29) (a) Bickelhaupt, F. M.; Baerends, E. J. *Rev. Comput. Chem.* **2000**, *15*, 1−86. (b) Te Velde, G.; Bickelhaupt, F. M.; Baerends, E. J.; Fonseca Guerra, C.; Van Gisbergen, J. A.; Snijders, J.; Ziegler, T. *J. Comput. Chem.* **2001**, *22*, 931.
(30) (a) Becke, A. D. *Phys. Rev. A: At., Mol., Opt. Phys.* **1988**, *38*, 3098. (b) Perdew, J. P. *Phys. Rev. B: Condens. Matter Mater. Phys.* **1986**, *33*, 8822.
(31) Snijders, J. G.; Baerends, E. J.; Vernoojs, P. *At. Data Nucl. Data Tables* **1981**, *26*, 483−509.
(32) Krijn, J.; Baerends, E. J. *Fit Functions in the HFS-Method; Internal Report* (in Dutch); Vrije Universiteit Amsterdam: The Netherlands, 1984.
(33) Van Lenthe, E.; Baerends, E. J.; Snijders, J. G. *J. Chem. Phys.* **1993**, 4597.
(34) Morokuma, K. *J. Chem. Phys.* **1971**, *55*, 1236.
(35) Ziegler, T.; Rauk, A. *Inorg. Chem.* **1979**, *18*, 1755.
(36) (a) Frenking, G.; Wichmann, K.; Fröhlich, N.; Loschen, C.; Lein, M.; Frunzke, J.; Rayón, M. *Coord. Chem. Rev.* **2003**, *238*−*239*, 55−91. (b) Lein, M.; Frenking, G. *Theory and Applications of Computational Chemistry: The First 40 Years*; Dykstra, C.E., Frenking, G., Kim, K.S., Scuseria, G.E., Eds.; Elsevier: Amsterdam, 2005; pp 367−414. (c) Krapp, A.; Bickelhaupt, F. M.; Frenking, G. *Chem.—Eur. J.* **2006**, *12*, 9196−9216. (d) Frenking, G.; Bickelhaupt, F. M. *The Chemical Bond. 1. Fundamental Aspects of Chemical Bonding*; Frenking, G., Shaik, S., Eds.; Wiley-VCH: Weinheim, 2014; pp 121−158.
(37) Mitoraj, M. P.; Michalak, A.; Ziegler, T. *J. Chem. Theory Comput.* **2009**, *5*, 962.
(38) Mitoraj, M. P.; Michalak, A. *Organometallics* **2007**, *26*, 6576.
(39) Mitoraj, M. P.; Michalak, A. *J. Mol. Model.* **2008**, *14*, 681.
(40) Jonas, V.; Frenking, G.; Reetz, M. T. *J. Am. Chem. Soc.* **1994**, *116*, 8741.
(41) (a) Dewar, M. J. S. *Bull. Soc. Chim. Fr.* **1951**, *18*, C79. (b) Chatt, J.; Duncanson, L. A. *J. Chem. Soc.* **1953**, 2929. (c) Frenking, G. *J. Organomet. Chem.* **2001**, *635*, 9. (d) Frenking, G. *Modern Coordination Chemistry: The Legacy of Joseph Chatt*; Leigh, G. J., Winterton, N., Eds.; The Royal Society: London, 2002; p 111.
(42) Frenking, G.; Antes, I.; Böhme, M.; Dapprich, S.; Ehlers, A. W.; Jonas, V.; Neuhaus, A.; Otto, M.; Stegmann, R.; Veldkamp, A.; Vyboishchikov, S. F. In *Reviews in Computational Chemistry*; Lipkowitz, K. B., Boyd, D. B., Eds.; VCH: New York, 1996; Vol. *8*, p 63.
(43) The smaller positive charge of Au (0.42) than Ag (0.51) in $[TM(cAAC)_2]$ can be explained with the higher electronegativity of gold than silver, which comes from relativistic effects. It has been shown that the electronegativity of Au increases due to relativistic effetcs by 0.54 on the Mulliken scale: Schwerdtfeger, P. *Chem. Phys. Lett.* **1991**, *183*, 457.
(44) (a) Pidun, U.; Frenking, G. *Organometallics* **1995**, *14*, 5325. (b) Pidun, U.; Frenking, G. *J. Organomet. Chem.* **1996**, *525*, 269. (c) Fischer, R. A.; Schulte, M. M.; Weiß, J.; Zsolnai, L.; Jacobi, A.; Huttner, G.; Frenking, G.; Boehme, C.; Vyboishchikov, S. F. *J. Am. Chem. Soc.* **1998**, *120*, 1237. (d) Frenking, G.; Wichmann, K.; Fröhlich, N.; Grobe, J.; Golla, W.; Le Van, D.; Krebs, B.; Läge, M. *Organometallics* **2002**, *21*, 2921. (e) Celik, M. A.; Sure, R.; Klein, S.; Kinjo, R.; Bertrand, G.; Frenking, G. *Chem.—Eur. J.* **2012**, *18*, 5676.
(45) (a) This point has also been stressed in Kraka, E.; Cremer, D. *ChemPhysChem* **2009**, *10*, 686. (b) The difference between the bond dissociation energy and the intrinsic interaction energy that should be used as measure for bond strength is pointed out in ref 36.
(46) Uddin, J.; Frenking, G. *J. Am. Chem. Soc.* **2001**, *123*, 1683.
(47) (a) Arduengo, A. J., III; Dias, H. V. R.; Calabrese, J. C.; Davidson, F. *Organometallics* **1993**, *12*, 3405. (b) Bonati, F.; Burini, A.; Bietroni, B. R.; Bovio, B. *J. Organomet. Chem.* **1989**, *375*, 147. (c) Britten, J. F.; Look, C. J. L.; Wang, Z. Z. *Acta Crystallogr., Sect. C: Cryst. Struct. Commun.* **1992**, C48.
(48) Nemcsok, D.; Wichmann, K.; Frenking, G. *Organometallics* **2004**, *23*, 3640.
(49) The NBO algorithm uses only those atomic valence orbitals of an atom for the bonding orbitals in a molecule that are occupied in the atomic ground state. The contribution of other basis functions are subject to a weighting factor that strongly reduces the mixing to the bonding orbitals. Thus, the (n)p AOs of the alkaline and earth alkaline atoms, the (n)d AOs of all main group atoms and the (n)p AOs of the transition metals are not treated as valence functions.
(50) (a) Schwerdtfeger, P. *The Chemical Bond. 1. Fundamental Aspects of Chemical Bonding*; Frenking, G., Shaik, S., Eds.; Wiley-VCH: Weinheim, 2014; p 383. (b) Pyykkö, P. *Annu. Rev. Phys. Chem.* **2012**, *63*, 4564. (c) Schwerdtfeger, P.; Lein, M. In *Gold Chemistry. Current Trends and Future Directions*; Mohr, F., Ed.; Wiley-VCH: Weinheim, 2009; p 183. (d) Schwerdtfeger, P. *Heteroatom Chem.* **2002**, *13*, 578. (e) Pyykkö, P. *Chem. Rev.* **1988**, *88*, 563.
(51) Antes, I.; Dapprich, S.; Frenking, G.; Schwerdtfeger, P. *Inorg. Chem.* **1996**, *35*, 2089.
(52) The notation $(cAAC)_2$ means that the two cAAC ligands were calculated at the frozen geometry of the complex $[TM(cAAC)_2]$. The bond dissociation energy D_e was calculated with respect to two separated cAAC ligands at their equilibrium geometry.